

MMA Regularization: Decorrelating Weights of Neural Networks by Maximizing the Minimal Angles

Zhennan Wang Canqun Xiang Wenbin Zou Chen Xu
Shenzhen University

{wangzhennan2017, xiangcanqun2018}@email.szu.edu.cn, {wzou, xuchen_szu}@szu.edu.cn

Abstract

The strong correlation between neurons or filters can significantly weaken the generalization ability of neural networks. Inspired by the well-known Tammes problem, we propose a novel diversity regularization method to address this issue, which makes the normalized weight vectors of neurons or filters distributed on a hypersphere as uniformly as possible, through *maximizing* the *minimal* pairwise *angles* (MMA). This method can easily exert its effect by plugging the MMA regularization term into the loss function with negligible computational overhead. The MMA regularization is simple, efficient, and effective. Therefore, it can be used as a basic regularization method in neural network training. Extensive experiments demonstrate that MMA regularization is able to enhance the generalization ability of various modern models and achieves considerable performance improvements on CIFAR100 and TinyImageNet datasets. In addition, experiments on face verification show that MMA regularization is also effective for feature learning.

1 Introduction

Although neural networks have achieved state-of-the-art results in a variety of tasks, they contain redundant neurons or filters due to the over-parametrization issue [37, 17], which is prevalent in networks [35]. The redundancy can lead to catching limited directions in feature space and poor generalization performance [23].

To address the redundancy problem and make neurons more discriminative, some methods are developed to encourage the angular diversity between pairwise weight vectors of neurons or filters in a layer, which can be categorized into the following three types. The first type reduces the redundancy by dropping some weights and then retraining them iteratively during optimization [31, 9, 32], which suffers from complex training scheme and very long training phase. The second type is the widely used orthogonal regularization [34, 48, 19, 47], which exploits a regularization term in loss function to enforce the pairwise weight vectors as orthogonal as possible. However, it has been proven that orthogonal regularization tends to group neurons closer, especially when the number of neurons is greater than the dimension [20], and therefore it only produces marginal improvements [31]. The third type also utilizes a regularization term but to encourage the weight vectors uniformly spaced through minimizing the hyperspherical potential energy [20, 18] inspired from the Thomson problem [43, 40]. Nonetheless, its disadvantage is that both the time complexity and the space complexity are very high [20], and it suffers from a huge number of local minima and stationary points due to its highly non-convex and non-linear objective function [18].

In this paper, we propose a simple, efficient, and effective method of angular diversity regularization which penalizes the minimum angles between pairwise weight vectors in each layer. Similar to the intuition of the third type mentioned above, the most diverse state is that the normalized weight vectors are distributed on a hypersphere uniformly. To model the criterion of uniformity, we employ the well-known Tammes problem, that is, to find the arrangement of n points on a unit sphere which maximizes the minimum distance between any two points [42, 25, 29, 22, 28]. However, the optimal

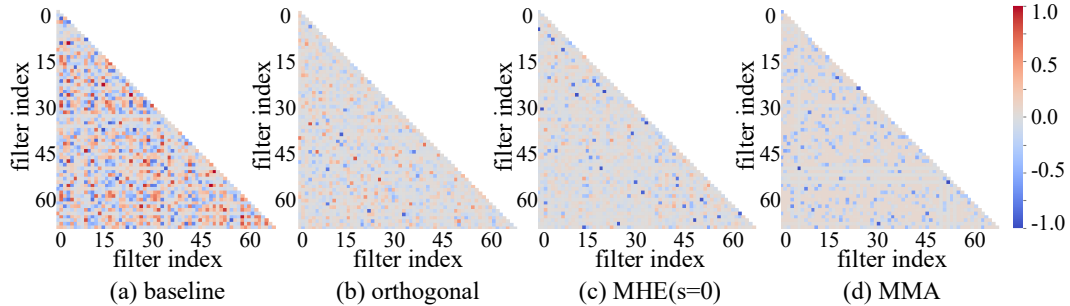


Figure 1: Comparison of filter cosine similarity from the first layer of VGG19-BN trained on CIFAR100 with several different methods of angular diversity regularization. The number of similarity values above 0.2 is 495 (baseline), 120 (orthogonal), 51 (MHE), 0 (MMA), demonstrating the effectiveness of MMA regularization.

solutions for the Tammes problem only exist for some combinations of the number of points n and dimensions d , which are collected on the N.J.A. Sloane’s homepage [39], and obtaining a uniform distribution for an arbitrary combination of n and d is still an open mathematical problem [25]. In this paper, we propose a numerical optimization method to get approximate solutions for the Tammes problem through *maximizing* the *minimal* pairwise *angles* between weight vectors, named as MMA for abbreviation. We further develop the MMA regularization for neural networks to promote the angular diversity of weight vectors in each layer and thus improve the generalization performance.

There are several advantages of MMA regularization: (a) As analyzed in Section 3.2, the gradient of MMA loss is stable and consistent, therefore it is easy to optimize and get near optimal solutions for the Tammes problem as shown in Table 1; (b) As verified in Table 3, the MMA regularization is easy to implement with negligible computational overhead, but with considerable performance improvements; (c) The MMA regularization is effective for both the hidden layers and the output layer, decorrelating the filters and enlarging the inter-class separability respectively. Therefore, it can be applied to multiple tasks, such as image classification and face verification demonstrated in this paper. To intuitively make sense of the effectiveness of MMA regularization, we visualize the cosine similarity of filters from the first layer of VGG19-BN trained on CIFAR100 in Figure 1. We compare several different methods of angular diversity regularization, including orthogonal regularization in [34], MHE regularization in [20], and the proposed MMA regularization. The results show that the MMA regularization gets the most uncorrelated filters. Besides, the MMA regularization keeps some negative correlations which have been verified to be beneficial for neural networks [5].

In summary, the main contributions of this paper are three-fold:

- We propose a numerical method for the Tammes problem, called MMA, which can get near optimal solutions under arbitrary combinations of the number of points and dimensions.
- We develop the novel MMA regularization which effectively promotes the angular diversity of weight vectors and therefore improves the generalization power of neural networks.
- Various experiments on multiple tasks show that MMA regularization is generally effective and can become a basic regularization method for training neural networks.

2 Related Work

To improve the generalization power of neural networks, many regularization methods have been proposed, such as weight decay [14], decoupled weight decay [21], weight elimination [46], nuclear norm [33], dropout [41], dropconnect [44], adding noise [2], and early stopping [24].

Recently, diversity-promoting regularization approaches are emerging. These methods mainly penalize the neural networks by adding a regularization term to the loss function. The regularization term either promotes the diversity of activations through minimizing the cross-covariance of hidden activations [6], or directly promotes the diversity of neurons or filters through enforcing the pairwise orthogonality [34, 48, 19, 47] or minimizing the global potential energy [20, 18]. For many tasks, these methods obtain marginal improvements [34, 31, 49, 4]. Another stream of approaches gets

comparatively diverse neurons or filters by cyclically dropping and relearning some of the weights [31, 9, 32], which leads to substantial performance gains, but suffers from complex training. In contrast, our proposed simple MMA regularization achieves significant performance improvements while employing the standard training procedures.

The most related work to our method is MHE [20], which targets the uniform distribution of normalized weight vectors on a hypersphere as well. However, the MHE is inspired by the Thomson problem [43] and models the criterion of uniformity as the minimum global potential energy, which suffers from high computational complexity and lots of local minima [18]. Inspired by the Tammes problem [42, 22], our proposed MMA regularization models the criterion as maximizing the minimum angles, that is the key reason why our method is more efficient and effective.

3 MMA Regularization

As our proposed regularization is inspired by the Tammes problem, we firstly analyze the Tammes problem and propose a numerical method called MMA which *maximizes* the *minimal* pairwise angles between the vectors. Then we make a comparison of several numerical methods for the Tammes problem by gradient analysis, which demonstrates the advantage of the proposed MMA. Finally, we develop a novel angular diversity regularization for neural networks by the proposed MMA.

3.1 The Tammes Problem and Proposed Numerical Method MMA

Construction of points spaced uniformly on a unit hypersphere $S^d \in R^d (d \in \{3, 4, 5, \dots\})$ is an important problem for various applications ranging from coding theory to computational geometry [29]. There are many ways to model the criterion of uniformity. One approach is to maximize the minimal pairwise distance between the points [29], i.e.

$$\max \min_{i,j,i \neq j} \|\hat{\mathbf{w}}_i - \hat{\mathbf{w}}_j\|, \quad s.t. \forall_i \quad \hat{\mathbf{w}}_i = \frac{\mathbf{w}_i}{\|\mathbf{w}_i\|} \quad (1)$$

where $\mathbf{w}_i \in R^{d \times 1}$ denotes the coordinate vector of the i -th point, $\hat{\mathbf{w}}$ denotes the l_2 -normalized vector, and the $\|\cdot\|$ denotes the Euclidean norm. This criterion means the points on a unit sphere are spaced uniformly when the minimal pairwise distance is maximized, which is known as the Tammes problem [42, 22] or the optimal spherical code [8, 39]. Denoting the dimension with d and the number of points with n , we firstly analyze the analytical solutions for the case of $d \geq n - 1$, and then propose the numerical solutions for the case of $d < n - 1$.

The analytical solutions for $d \geq n - 1$. As the distance between any two points on a unit hypersphere is inversely proportional to the cosine similarity, the Tammes problem is equivalent to minimize the maximal pairwise cosine similarity, i.e.

$$\min \max_{i,j,i \neq j} \hat{\mathbf{w}}_i \cdot \hat{\mathbf{w}}_j, \quad s.t. \forall_i \quad \hat{\mathbf{w}}_i = \frac{\mathbf{w}_i}{\|\mathbf{w}_i\|} \quad (2)$$

The maximum of $\hat{\mathbf{w}}_i \cdot \hat{\mathbf{w}}_j$ must be larger than the average. Therefore, the minimum is derived as:

$$n(n-1) \max_{i,j,i \neq j} \hat{\mathbf{w}}_i \cdot \hat{\mathbf{w}}_j \geq \sum_{i,j,i \neq j} \hat{\mathbf{w}}_i \cdot \hat{\mathbf{w}}_j = \left\| \sum_i \hat{\mathbf{w}}_i \right\|^2 - \sum_i \|\hat{\mathbf{w}}_i\|^2 = \left\| \sum_i \hat{\mathbf{w}}_i \right\|^2 - n \geq -n \quad (3)$$

Therefore, the minimum of maximal pairwise cosine similarity is $-\frac{1}{n-1}$, which can be reached when all pairwise angles between the points are equal to each other, and the sum of all vectors is a zero vector. This criterion has a matrix form:

$$\mathbf{C} = \hat{\mathbf{W}} \hat{\mathbf{W}}^T = \begin{bmatrix} 1 & -\frac{1}{n-1} & \cdots & -\frac{1}{n-1} \\ -\frac{1}{n-1} & 1 & \ddots & \vdots \\ \vdots & \ddots & \ddots & -\frac{1}{n-1} \\ -\frac{1}{n-1} & \cdots & -\frac{1}{n-1} & 1 \end{bmatrix}, \quad s.t. \forall_i \quad \hat{\mathbf{W}}_i = \frac{\mathbf{w}_i^T}{\|\mathbf{w}_i\|} \quad (4)$$

where $\hat{\mathbf{W}} \in R^{n \times d}$ denotes the set of l_2 -normalized points. According to the matrix theory, the eigenvalues of matrix \mathbf{C} are $\lambda_1 = 0$ with algebraic multiplicity of 1 and $\lambda_2 = \frac{n}{n-1}$ with algebraic multiplicity of $n - 1$. As all the eigenvalues of \mathbf{C} are greater than or equal to zero, \mathbf{C} is a semi-positive definite matrix. According to the spectral theorem [3], $\hat{\mathbf{W}}$ can be gotten through the eigendecomposition of \mathbf{C} , which is the analytical solution for the Tammes problem. However, since the rank of \mathbf{C} is $n - 1$, the rank of $\hat{\mathbf{W}}$ and the minimum dimension of the points are also $n - 1$. Therefore, this analytical solution only exists for the case of $d \geq n - 1$.

The numerical solutions for $d < n - 1$. So far, under the case of $d < n - 1$, the analytical solutions for the Tammes problem only exist for some combinations of n and d [39]. For most combinations, the optimal solutions do not exist. Consequently, numerical methods are used to get approximate solutions.

As the objective (Equation 1) of Tammes problem is not globally differentiable [30], the conventional solution [1] alternatively optimizes a differentiable potential energy function to get the approximate solutions, as discussed in next subsection. Nonetheless, with the help of SGD [36] and modern automatic differentiation library [27], we can now directly use Equation (1) to implement optimization and get the approximate solutions. However, the calculation of Euclidean length is expensive. Alternatively, as mentioned in Equation (2), we can use the cosine similarity as the objective function, called cosine loss, which is formulated as follows:

$$l_{\text{cosine}} = \frac{1}{n} \sum_{i=1}^n \max_{j, j \neq i} \text{Cos}_{ij}, \quad \text{Cos} = \hat{\mathbf{W}} \hat{\mathbf{W}}^T, \quad s.t. \forall_i \quad \hat{\mathbf{W}}_i = \frac{\mathbf{w}_i^T}{\|\mathbf{w}_i\|} \quad (5)$$

where $\text{Cos} \in R^{n \times n}$ denotes the cosine similarity matrix of the points. Employing the global maximum similarity as Equation (2) is inefficient, as it only updates the closest pair of points. Therefore, we alternatively use the average of each vector's maximum similarity.

The cosine loss can be optimized quickly taking the advantage of matrix form. However, we find this loss is hard to converge, especially for the case that \mathbf{w}_i is very close to \mathbf{w}_j , which is very prevalent in neural networks [35]. As analyzed in next subsection, this is because the gradient is too small to cover random fluctuations during the optimization. Gaining insight from the ArcFace [7], we propose the angular version of cosine loss as the object function:

$$l_{\text{MMA}} = -\frac{1}{n} \sum_{i=1}^n \min_{j, j \neq i} \theta_{ij}, \quad \theta = \arccos(\hat{\mathbf{W}} \hat{\mathbf{W}}^T), \quad s.t. \forall_i \quad \hat{\mathbf{W}}_i = \frac{\mathbf{w}_i^T}{\|\mathbf{w}_i\|} \quad (6)$$

where $\theta \in R^{n \times n}$ denotes the pairwise angle matrix. As this loss *maximizes* the *minimal* pairwise angles, we name it MMA loss for abbreviation. The MMA loss is very efficient and robust for optimization, so it is easy to get near optimal numerical solutions for the Tammes problem. Besides, it can also get close solutions for the case $d \geq n - 1$, which is validated in Section 4. In next subsection, we demonstrate the advantage of the proposed MMA loss through gradient analysis and comparison.

3.2 The Gradient Analysis

In this subsection, we analyze and compare the gradients of loss functions generating approximate solutions for uniformly spaced points. To simplify the derivation, we only consider the norm of the gradient of the core function, composing the summation in loss functions, w.r.t. corresponding weight vector \mathbf{w}_i . For intuitive comparison, the analysis results are presented in Figure 2.

Corresponding to the cosine loss referred to Equation (5), the gradient norm is derived as follows:

$$\left\| \frac{\partial \text{Cos}_{ij}}{\partial \mathbf{w}_i} \right\| = \left\| \frac{\partial \left(\frac{\mathbf{w}_i^T \mathbf{w}_j}{\|\mathbf{w}_i\| \|\mathbf{w}_j\|} \right)}{\partial \mathbf{w}_i} \right\| = \frac{\|(I - M_{\mathbf{w}_i})\mathbf{w}_j\|}{\|\mathbf{w}_i\| \|\mathbf{w}_j\|} = \frac{\|\mathbf{w}_j\| \sin \theta_{ij}}{\|\mathbf{w}_i\| \|\mathbf{w}_j\|} = \frac{\sin \theta_{ij}}{\|\mathbf{w}_i\|}, \quad M_{\mathbf{w}_i} = \frac{\mathbf{w}_i \mathbf{w}_i^T}{\|\mathbf{w}_i\|^2} \quad (7)$$

where $M_{\mathbf{w}_i}$ represents the projection matrix of \mathbf{w}_i . From the above derivation and Figure 2, we can see that the gradient norm is very small when pairwise angle is close to zero. That is why the cosine loss is hard to converge for the case that \mathbf{w}_i and \mathbf{w}_j are close to each other, as experimented in Section 4. Next, we derive the gradient norm corresponding to the MMA loss referred to Equation (6):

$$\left\| \frac{\partial \theta_{ij}}{\partial \mathbf{w}_i} \right\| = \left\| \frac{\partial \theta_{ij}}{\partial \cos \theta_{ij}} \frac{\partial \cos \theta_{ij}}{\partial \mathbf{w}_i} \right\| = \frac{1}{\sin \theta_{ij}} \frac{\sin \theta_{ij}}{\|\mathbf{w}_i\|} = \frac{1}{\|\mathbf{w}_i\|} \quad (8)$$

Compared to the gradient norm corresponding to the cosine loss, as referred to Equation (7), the gradient norm corresponding to the MMA loss is independent of the pairwise angle θ_{ij} , so it would not encounter the very small gradient even though θ_{ij} is zero. Figure 2 shows that the gradient norm

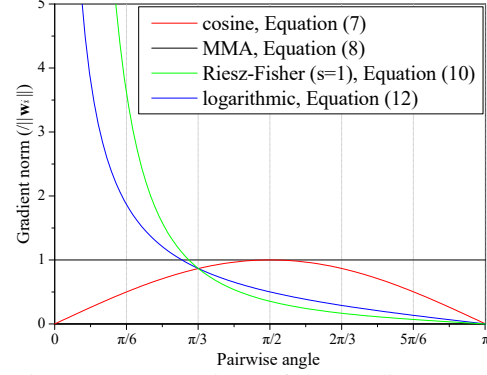


Figure 2: Comparison of the gradient norm changed with pairwise angle. The gradient of MMA loss is stable and consistent.

corresponding to MMA loss is stable and consistent. Therefore, the MMA loss is easy to optimize and get near optimal solutions for the Tammes problem, verified by experiments in Section 4.

In addition to the above two loss functions, we also analyze the Riesz-Fisher loss [29] and the logarithmic loss [29] which are often used to get uniformly distributed points on a hypersphere. The philosophy behind the two loss functions is that the points on a hypersphere are uniformly spaced when the potential energy is minimum, and both of them are formulated as kernel functions of the potential energy. The Riesz-Fisher loss and the corresponding gradient norm are:

$$l_{RF} = \frac{1}{n(n-1)} \sum_{i \neq j} \|\hat{\mathbf{w}}_i - \hat{\mathbf{w}}_j\|^{-s}, \quad s > 0 \quad (9)$$

$$\left\| \frac{\partial \|\hat{\mathbf{w}}_i - \hat{\mathbf{w}}_j\|^{-s}}{\partial \mathbf{w}_i} \right\| = \frac{s}{\|\mathbf{w}_i\|} \frac{\cos \frac{\theta_{ij}}{2}}{(2 \sin \frac{\theta_{ij}}{2})^{s+1}} \quad (10)$$

where s is a hyperparameter, and is set to 1 in Figure 2 for easy comparison. The logarithmic loss and the corresponding gradient norm are:

$$l_{log} = -\frac{1}{n(n-1)} \sum_{i \neq j} \log \|\hat{\mathbf{w}}_i - \hat{\mathbf{w}}_j\| \quad (11)$$

$$\left\| \frac{\partial \log \|\hat{\mathbf{w}}_i - \hat{\mathbf{w}}_j\|}{\partial \mathbf{w}_i} \right\| = \frac{1}{\|\mathbf{w}_i\|} \frac{\cos \frac{\theta_{ij}}{2}}{(2 \sin \frac{\theta_{ij}}{2})} \quad (12)$$

Due to the limited space, more details of derivation are presented in the supplementary material. As visualized in Figure 2, the Riesz-Fisher loss and logarithmic loss have similar properties: the gradient norm is sharp around angles near zero and drops rapidly as the angle increases. Besides, the greater the s of Riesz-Fisher loss is, the sharper the gradient norm becomes. The very large gradient norm around angles near zero can cause instability and prevent the normal learning of neural networks, and the very small gradient norm around angles away from zero makes the updates inefficient. We argue that is why the two loss functions just get inaccurate solutions for the Tammes problem in Section 4 and perform not so good in terms of accuracy in Table 3.

3.3 MMA Regularization for Neural Networks

In this subsection, we develop the MMA regularization for neural networks, which promotes the learning towards uniformly distributed weight vectors in angular space. For $d \geq n - 1$, we can employ the cosine similarity matrix in Equation (4) to constrain the weights. However, as the MMA loss can generate accurate approximate solutions in any case and is easy to implement, we uniformly exploit the MMA loss referred to Equation (6) as the angular regularization:

$$l_{MMA_regularization} = \lambda \sum_{i=1}^L l_{MMA}(\mathbf{W}_i) \quad (13)$$

where λ denotes regularization coefficient, L denotes the total number of layers, including convolutional layers and fully connected layers, and \mathbf{W}_i denotes the weight matrix of the i -th layer with each row denoting a vectorized filter or neuron.

The MMA regularization is complementary and orthogonal to weight decay [14]. Weight decay regularizes the Euclidean norm of weight vectors, while MMA regularization promotes the direction diversity of weight vectors. MMA regularization can be applied into both hidden layers and output layer. For hidden layers, MMA regularization can reduce the redundancy of filters, which is very common in neural networks [35]. Consequently, the unnecessary overlap in the features captured by the network's filters is diminished. For output layer, MMA regularization can maximize the inter-class separability and therefore enhance the discriminative power of neural networks.

4 Experiments for the Tammes Problem

This section compares several numerical methods for the Tammes problem, measured by the minimum angle, as shown in Table 1. The first column denotes the dimension d and the second column denotes the number of points n . The third column refers the minimal pairwise angles of the optimal solutions collected in [39]. The rest columns are the minimum angle obtained by several different numerical methods, including MMA loss in Equation (6), cosine loss in Equation (5), Riesz-Fisher loss with $s = 2$ in Equation (9), and logarithmic loss in Equation (11). The weights are initialized with values drawn from the standard normal distribution and then optimized by SGD [36] with 10000 iterations. The initial learning rate is set to 0.1 and reduced by a factor of 5 once learning stagnates, and the momentum is set to 0.9.

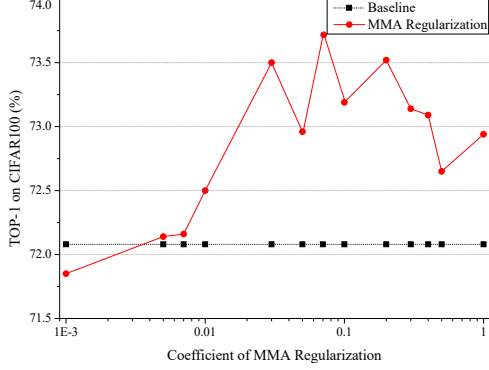


Figure 3: Coefficient tuning for VGG19-BN.

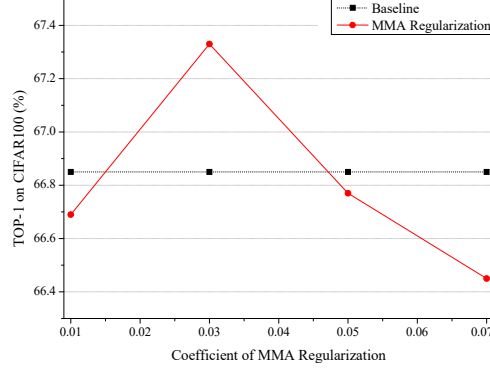


Figure 4: Coefficient tuning for ResNet20.

For $d \geq n - 1$, as analyzed in Section 3.1, each pairwise angle of optimal solutions is $\arccos(-\frac{1}{n-1})$, verified by the second row ($d=3, n=4$), the fifth row ($d=4, n=5$), and the ninth row ($d=5, n=6$), from which we can observe that the optimal solutions can be easily achieved by any of the four numerical methods. For $d < n - 1$, all the numerical solutions are more or less prone to be worse than the optimal solutions. However, the MMA loss can robustly obtain the closest solutions to the optimal. The cosine loss can also achieve very close solutions, but it is not robust for the cases of too many

points like the third row ($d=3, n=30$), the forth row ($d=3, n=130$), and the eighth row ($d=4, n=600$). This is due to the too small gradient as analyzed in Section 3.2. The Riesz-Fisher loss and the logarithmic loss are also robust, but they converge to solutions far from the optimal.

Table 1: Minimum angle (degree) obtained by several different loss functions for the Tammes problem. The best results are highlighted in bold.

d	n	optimal	l_{MMA}	l_{cosine}	l_{RF}	l_{log}
3	4	109.5	109.5	109.5	109.4	109.5
3	30	38.6	38.5	0	34.9	35.4
3	130	18.5	17.6	0	12.6	16.7
4	5	104.5	104.5	104.5	104.5	104.5
4	30	54.3	54.0	53.7	49.3	48.6
4	130	33.4	32.0	32.1	27.9	27.2
4	600	19.8	19.3	0	15.9	13.1
5	6	101.5	101.5	101.5	101.2	101.5
5	30	65.6	65.5	64.0	57.1	60.0
5	130	43.8	42.9	42.5	35.8	35.6

5 Experiments on Image Classification

5.1 Implementation Settings

We conduct image classification experiments on CIFAR100 [13] and TinyImageNet [15]. For both datasets, we follow the simple data augmentation in [16]. We employ various classic networks as the backbone networks, including ResNet56 [10], VGG19 [38] with batch normalization [12] denoted by VGG19-BN, VGG16 with batch normalization denoted by VGG16-BN, WideResNet [50] with 16 layers and a widen factor of 8 denoted by WRN-16-8, and DenseNet [11] with 40 layers and a growth rate of 12 denoted by DenseNet-40-12. We denote the corresponding MMA regularization version of models by X-MMA. For fair comparison, not only the X-MMA models but also the corresponding backbones are trained from scratch, so our results may be slightly different from the ones presented in the original papers due to different random seeds and hardware settings. For CIFAR100, the hyperparameters and settings are the same as the original papers. For TinyImageNet, we follow the settings in [45]. Besides, all the random seeds are fixed, so the experiments are reproducible and comparisons are absolutely fair. Moreover, in order to reduce the variance of evaluation, we employ the average accuracy of last five epochs as the evaluation criterion.

5.2 Ablation Study

To understand the behavior of MMA regularization, we conduct comprehensive ablation experiments on CIFAR100. Except otherwise noted, we use the VGG19-BN to implement ablation experiments.

Impact of the hyperparameter. The MMA regularization coefficient λ is the only hyperparameter. As the skip connections have implicitly promoted the angular diversity of neurons [26], we separately select the VGG19-BN and ResNet20 to investigate the impact of different coefficients for models without and with skip connections, as shown in Figure 3 and Figure 4 respectively. From both of the figures, we can see that the effect of MMA regularization with too small coefficients is not

obvious. However, too large coefficients improve slightly or even decrease the performance. This is because too strong regularization prevents the normal learning of neural networks to some extent. For the VGG19-BN, MMA regularization is not very sensitive to the hyperparameter and works well from 0.03 to 0.2, therefore proving the effectiveness of MMA regularization. For the Resnet20, it is sensitive because of the skip connections. In the following experiments, we set MMA regularization coefficient to 0.07 for VGG models and 0.03 for models with skip connections.

Effectiveness for hidden layers and output layer. The MMA regularization is applicable to both the hidden layers and the output layer. In Table 2, we study the effect of MMA regularization applied to hidden layers (*hidden*) and all layers (*hidden+output*). The results show that the *hidden* version improves over the VGG19-BN baseline with a considerable margin and, moreover, the *hidden+output* version improves the performance further. This indicates that the MMA regularization is effective for both the hidden layers and the output layer, and the effects can be accumulated. As analyzed in Section 3.3, the effectiveness for hidden layers comes from decorrelating the filters or neurons, and the effectiveness for output layer comes from enlarging the inter-class separability.

Table 2: Accuracy (%) of applying MMA regularization to different layers.

Model	TOP-1	TOP-5
baseline	72.08	90.5
hidden	73.45	90.91
hidden+output	73.73	91.21

Comparison with other angular regularization. This section compares several angular regularization from the perspective of calculating time per batch, occupied memory, accuracy, and the minimum pairwise angles of several layers, as shown in Table 3. Besides the MMA regularization, we also consider the MHE [20] regularization and the widely used orthogonal regularization [34, 48, 19, 47] which also penalize the pairwise angles. The MHE actually takes the Riesz-Fisher loss ($s>0$) or logarithmic loss ($s=0$) to implement regularization [20]. The orthogonal regularization promotes all the pairwise weight vectors to be orthogonal. Here, we adopt the orthogonal regularization in [34]:

$$l_{orthogonal} = \frac{\lambda}{2} \sum_{i=1}^L \|\hat{\mathbf{W}}_i \hat{\mathbf{W}}_i^T - \mathbf{I}\|_F^2 \quad (14)$$

where $\hat{\mathbf{W}}_i$ denotes the l_2 -normalized weight matrix of the i -th layer, \mathbf{I} denotes identity matrix, and $\|\cdot\|_F$ denotes the Frobenius norm.

Table 3: Comparison of several different methods of angular regularization. The MMA achieves the most diverse filters and highest accuracy with negligible computational overhead.

Regularization	Time(s) /Batch	Memory (MiB)	Accuracy (%)		Minimum Angle (degree)			
			TOP-1	TOP-5	L3-3	L4-3	L5-3	Classify
baseline	0.070	1127	72.08	90.50	70.1	16.0	30.8	54.0
MMA	0.095	1229	73.73	91.21	85.7	84.7	85.3	84.9
MHE($s=2$)	0.259	5551	71.91	90.76	74.2	58.1	68.5	71.3
MHE($s=0$)	0.253	5551	72.08	90.72	69.6	48.6	57.8	63.4
orthogonal	0.096	1237	72.83	90.98	79.3	75.3	81.2	63.1

The coefficient is set to 0.07 for MMA, 1.0 for MHE [20], and 0.0001 for orthogonal regularization [47]. Due to the limit of GPU memory, we employ the mini-batch version of MHE [20], which iteratively takes a random batch (here, 30% of the total) of weight vectors to calculate the loss. For the comparison of minimal pairwise angle, we select the third layer of the third block, forth block, and fifth block, and the classification layer, which are denoted by *L3-3*, *L4-3*, *L5-3*, and *Classify* respectively. These experiments are based on PyTorch [27] and NVIDIA GeForce GTX 1080 GPU.

Compared to the baseline, the MMA regularization and orthogonal regularization slightly increase the calculating time and occupied memory. However, the MHE regularization greatly increases that due to the computation of all the pairwise distances. In terms of accuracy, the MMA regularization improves over the baseline by a substantial margin. The orthogonal regularization is also effective but inferior to the MMA regularization. The MHE regularization is just comparable to the baseline, which may be because of the unstable gradient as analyzed in Section 3.2. We also observe that there is a strong link between the minimal pairwise angles in hidden layers and the accuracy—the larger the minimal angles, the higher the accuracy. This is because the larger minimal angle means the more diverse filters which would improve the generalizability of models. The MMA regularization is also the most effective to enlarge the minimal pairwise angle of classification layer, which would increase the inter-class separability and enhance the discriminative power of neural networks. More plots and comparison of the minimal pairwise angles are shown in the supplementary material.

5.3 Results and Analysis

We firstly compare various modern architectures with their MMA regularization versions on CIFAR100. From the results shown in Table 4, we can see that the X-MMA can typically improve the corresponding backbone models. Especially, MMA regularization improves the TOP-1 accuracy of VGG19-BN by 1.65%. MMA regularization is also able to robustly improve the performance of models with skip connections like ResNet, DenseNet, and WideResNet, although the improvement is not as distinct as in VGG. This is because the skip connections have implicitly reduced feature correlations to some extent [26].

Table 4: Accuracy (%) on CIFAR100.

Model	TOP-1	TOP-5
ResNet56	70.39	91.12
ResNet56-MMA	70.90	91.25
VGG19-BN	72.08	90.50
VGG19-BN-MMA	73.73	91.21
WRN-16-8	78.97	94.84
WRN-16-8-MMA	79.34	95.05
DenseNet-40-12	73.98	92.74
DenseNet-40-12-MMA	74.61	92.77

Table 5: Accuracy (%) on TinyImageNet.

Model	TOP-1	TOP-5
ResNet56	54.80	78.71
ResNet56-MMA	55.24	78.92
VGG16-BN	62.16	82.41
VGG16-BN-MMA	63.37	82.68

To further demonstrate the consistency of MMA’s superiority, we also evaluate the MMA regularization with ResNet56 and VGG16-BN on TinyImageNet, with the coefficient of 0.01 and 0.07 respectively. The results are reported in Table 5, where the X-MMA models successfully outperform the original backbones on both Top-1 and Top-5 accuracy. It is worth emphasizing that the X-MMA models achieve the improvements with quite

negligible computational overhead and without modifying the original network architecture.

6 ArcFace+: Applying MMA Regularization to ArcFace

ArcFace [7] is one of the state-of-the-art face verification methods, which proposes an additive angular margin between the learned feature and the target weight vector in the classification layer. This method essentially encourages intra-class feature compactness by promoting the learned features close to the target weight vectors. As analyzed in Section 3.3, MMA regularization can achieve diverse weight vectors and therefore improve inter-class separability for classification layer. Consequently, the MMA regularization is complementary to the objective of ArcFace and should boost accuracy further. Motivated by this analysis, we propose ArcFace+ by applying MMA Regularization to ArcFace. The objective function of ArcFace+ is defined as:

$$l_{arcface+} = l_{arcface}(m) + \lambda l_{MMA}(\mathbf{W}_{classify}) \quad (15)$$

where m is the angular margin of ArcFace, λ is the regularization coefficient, and $\mathbf{W}_{classify}$ is the weight matrix of classification layer.

For fair comparison, both the ArcFace and ArcFace+ are trained from scratch, therefore our results of the ArcFace may be slightly different from the ones presented in the original paper due to different settings and hardware. The implementation settings are detailed in the supplementary material.

From the results shown in Table 6, we can see that the ArcFace+ outperforms ArcFace across all the three verification datasets by margins which are very significant in the field of face verification. This comparison validates the effectiveness of MMA regularization in feature learning. Note that these results are obtained with the default coefficient 0.03, we argue the results may be better with hyperparameter tuning.

Table 6: Comparison of verification results (%).

Method	LFW	CFP-FP	AgeDB-30
ArcFace	99.35	95.30	94.62
ArcFace+	99.45	95.59	95.15

7 Conclusion

In this paper, we propose a novel regularization method for neural networks, called MMA regularization, to encourage the angularly uniform distribution of weight vectors and therefore decorrelate the filters or neurons. The MMA regularization has stable and consistent gradient, and is easy to implement with negligible computational overhead, and is effective for both the hidden layers and the output layer. Extensive experiments on image classification demonstrate that the MMA regularization is able to enhance the generalization power of neural networks by considerable improvements. Moreover, MMA regularization is also effective for feature learning with significant margins, due to enlarging the inter-class separability. As the MMA can be viewed as a basic regularization method for neural networks, we will explore the effectiveness of MMA regularization on other tasks, such as object detection, object tracking, and image captioning, etc.

References

- [1] Patrick Guy Adams. A numerical approach to tamme’s problem in euclidean n-space. 1997.
- [2] Guozhong An. The effects of adding noise during backpropagation training on a generalization performance. *Neural computation*, 8(3):643–674, 1996.
- [3] Sheldon Jay Axler. *Linear algebra done right*, volume 2. Springer, 1997.
- [4] Andrew Brock, Theodore Lim, James M Ritchie, and Nick Weston. Neural photo editing with introspective adversarial networks. *arXiv preprint arXiv:1609.07093*, 2016.
- [5] Mircea I Chelaru and Valentin Dragoi. Negative correlations in visual cortical networks. *Cerebral Cortex*, 26(1):246–256, 2016.
- [6] Michael Cogswell, Faruk Ahmed, Ross Girshick, Larry Zitnick, and Dhruv Batra. Reducing overfitting in deep networks by decorrelating representations. *arXiv preprint arXiv:1511.06068*, 2015.
- [7] Jiankang Deng, Jia Guo, Niannan Xue, and Stefanos Zafeiriou. Arcface: Additive angular margin loss for deep face recognition. In *Proceedings of the IEEE Conference on Computer Vision and Pattern Recognition*, pages 4690–4699, 2019.
- [8] Thomas Ericson and Victor Zinoviev. *Codes on Euclidean spheres*. Elsevier, 2001.
- [9] Song Han, Jeff Pool, Sharan Narang, Huizi Mao, Enhao Gong, Shijian Tang, Erich Elsen, Peter Vajda, Manohar Paluri, John Tran, et al. Dsd: Dense-sparse-dense training for deep neural networks. *arXiv preprint arXiv:1607.04381*, 2016.
- [10] Kaiming He, Xiangyu Zhang, Shaoqing Ren, and Jian Sun. Deep residual learning for image recognition. In *Proceedings of the IEEE conference on computer vision and pattern recognition*, pages 770–778, 2016.
- [11] Gao Huang, Zhuang Liu, Laurens Van Der Maaten, and Kilian Q Weinberger. Densely connected convolutional networks. In *Proceedings of the IEEE conference on computer vision and pattern recognition*, pages 4700–4708, 2017.
- [12] Sergey Ioffe and Christian Szegedy. Batch normalization: Accelerating deep network training by reducing internal covariate shift. *arXiv preprint arXiv:1502.03167*, 2015.
- [13] Alex Krizhevsky and Geoffrey Hinton. Learning multiple layers of features from tiny images. Technical report, Citeseer, 2009.
- [14] Anders Krogh and John A Hertz. A simple weight decay can improve generalization. In *Advances in neural information processing systems*, pages 950–957, 1992.
- [15] Ya Le and Xuan Yang. Tiny imagenet visual recognition challenge. *CS 231N*, 2015.
- [16] Chen-Yu Lee, Saining Xie, Patrick Gallagher, Zhengyou Zhang, and Zhuowen Tu. Deeply-supervised nets. In *Artificial Intelligence and Statistics*, pages 562–570, 2015.
- [17] Hao Li, Asim Kadav, Igor Durdanovic, Hanan Samet, and Hans Peter Graf. Pruning filters for efficient convnets. 2017.
- [18] Rongmei Lin, Weiyang Liu, Zhen Liu, Chen Feng, Zhiding Yu, James M Rehg, Li Xiong, and Le Song. Regularizing neural networks via minimizing hyperspherical energy. *arXiv preprint arXiv:1906.04892*, 2020.
- [19] Weiyang Liu, Yan-Ming Zhang, Xingguo Li, Zhiding Yu, Bo Dai, Tuo Zhao, and Le Song. Deep hyperspherical learning. In *Advances in neural information processing systems*, pages 3950–3960, 2017.
- [20] Weiyang Liu, Rongmei Lin, Zhen Liu, Lixin Liu, Zhiding Yu, Bo Dai, and Le Song. Learning towards minimum hyperspherical energy. In *Advances in neural information processing systems*, pages 6222–6233, 2018.

- [21] Ilya Loshchilov and Frank Hutter. Decoupled weight decay regularization. *arXiv preprint arXiv:1711.05101*, 2017.
- [22] L Lovisolo and EAB Da Silva. Uniform distribution of points on a hyper-sphere with applications to vector bit-plane encoding. *IEE Proceedings-Vision, Image and Signal Processing*, 148(3):187–193, 2001.
- [23] Ari S Morcos, David GT Barrett, Neil C Rabinowitz, and Matthew Botvinick. On the importance of single directions for generalization. *arXiv preprint arXiv:1803.06959*, 2018.
- [24] Nelson Morgan and Hervé Bourlard. Generalization and parameter estimation in feedforward nets: Some experiments. In *Advances in neural information processing systems*, pages 630–637, 1990.
- [25] Oleg R Musin and Alexey S Tarasov. The tammes problem for $n=14$. *Experimental Mathematics*, 24(4):460–468, 2015.
- [26] A Emin Orhan and Xaq Pitkow. Skip connections eliminate singularities. *arXiv preprint arXiv:1701.09175*, 2017.
- [27] Adam Paszke, Sam Gross, Francisco Massa, Adam Lerer, James Bradbury, Gregory Chanan, Trevor Killeen, Zeming Lin, Natalia Gimelshein, Luca Antiga, et al. Pytorch: An imperative style, high-performance deep learning library. In *Advances in Neural Information Processing Systems*, pages 8024–8035, 2019.
- [28] Federico Pernici, Matteo Bruni, Claudio Baccchi, and Alberto Del Bimbo. Fix your features: Stationary and maximally discriminative embeddings using regular polytope (fixed classifier) networks. *arXiv preprint arXiv:1902.10441*, 2019.
- [29] Marko D Petković and Nenad Živić. The feket problem and construction of the spherical coverage by cones. *Facta universitatis-series: Mathematics and Informatics*, 28(4):393–402, 2013.
- [30] János D Pintér. Globally optimized spherical point arrangements: model variants and illustrative results. *Annals of Operations Research*, 104(1-4):213–230, 2001.
- [31] Aaditya Prakash, James Storer, Dinei Florencio, and Cha Zhang. Repr: Improved training of convolutional filters. In *Proceedings of the IEEE Conference on Computer Vision and Pattern Recognition*, pages 10666–10675, 2019.
- [32] Siyuan Qiao, Zhe Lin, Jianming Zhang, and Alan L Yuille. Neural rejuvenation: Improving deep network training by enhancing computational resource utilization. In *Proceedings of the IEEE Conference on Computer Vision and Pattern Recognition*, pages 61–71, 2019.
- [33] Benjamin Recht, Maryam Fazel, and Pablo A Parrilo. Guaranteed minimum-rank solutions of linear matrix equations via nuclear norm minimization. *SIAM review*, 52(3):471–501, 2010.
- [34] Pau Rodríguez, Jordi González, Guillem Cucurull, Josep M. Gonfaus, and F. Xavier Roca. Regularizing cnns with locally constrained decorrelations. In *5th International Conference on Learning Representations, ICLR 2017, Conference Track Proceedings*, 2017.
- [35] Aruni RoyChowdhury, Prakhar Sharma, and Erik G. Learned-Miller. Reducing duplicate filters in deep neural networks. In *NIPS workshop on Deep Learning: Bridging Theory and Practice*, 2017.
- [36] David E Rumelhart, Geoffrey E Hinton, and Ronald J Williams. Learning representations by back-propagating errors. *nature*, 323(6088):533–536, 1986.
- [37] Wenling Shang, Kihyuk Sohn, Diogo Almeida, and Honglak Lee. Understanding and improving convolutional neural networks via concatenated rectified linear units. In *international conference on machine learning*, pages 2217–2225, 2016.
- [38] Karen Simonyan and Andrew Zisserman. Very deep convolutional networks for large-scale image recognition. *arXiv preprint arXiv:1409.1556*, 2014.

- [39] N.J.A. Sloane, R.H. Hardin, W.D. Smith, et al. Tables of spherical codes. See <http://neilsloane.com/packings/>, 2000.
- [40] Steve Smale. Mathematical problems for the next century. *The mathematical intelligencer*, 20(2):7–15, 1998.
- [41] Nitish Srivastava, Geoffrey Hinton, Alex Krizhevsky, Ilya Sutskever, and Ruslan Salakhutdinov. Dropout: a simple way to prevent neural networks from overfitting. *The journal of machine learning research*, 15(1):1929–1958, 2014.
- [42] Pieter Merkus Lambertus Tammes. On the origin of number and arrangement of the places of exit on the surface of pollen-grains. *Recueil des travaux botaniques néerlandais*, 27(1):1–84, 1930.
- [43] Joseph John Thomson. Xxiv. on the structure of the atom: an investigation of the stability and periods of oscillation of a number of corpuscles arranged at equal intervals around the circumference of a circle; with application of the results to the theory of atomic structure. *The London, Edinburgh, and Dublin Philosophical Magazine and Journal of Science*, 7(39): 237–265, 1904.
- [44] Li Wan, Matthew Zeiler, Sixin Zhang, Yann Le Cun, and Rob Fergus. Regularization of neural networks using dropconnect. In *International conference on machine learning*, pages 1058–1066, 2013.
- [45] Chaoqi Wang, Guodong Zhang, and Roger Grosse. Picking winning tickets before training by preserving gradient flow. *arXiv preprint arXiv:2002.07376*, 2020.
- [46] Andreas S Weigend, David E Rumelhart, and Bernardo A Huberman. Generalization by weight-elimination with application to forecasting. In *Advances in neural information processing systems*, pages 875–882, 1991.
- [47] Di Xie, Jiang Xiong, and Shiliang Pu. All you need is beyond a good init: Exploring better solution for training extremely deep convolutional neural networks with orthonormality and modulation. In *Proceedings of the IEEE Conference on Computer Vision and Pattern Recognition*, pages 6176–6185, 2017.
- [48] Pengtao Xie, Yuntian Deng, Yi Zhou, Abhimanu Kumar, Yaoliang Yu, James Zou, and Eric P Xing. Learning latent space models with angular constraints. In *Proceedings of the 34th International Conference on Machine Learning-Volume 70*, pages 3799–3810. JMLR. org, 2017.
- [49] Pengtao Xie, Barnabas Poczos, and Eric P Xing. Near-orthogonality regularization in kernel methods. In *UAI*, volume 3, page 6, 2017.
- [50] Sergey Zagoruyko and Nikos Komodakis. Wide residual networks. *arXiv preprint arXiv:1605.07146*, 2016.

Supplementary Material

A Detail Derivation of Equation (10) and Equation (12)

The detail derivation of Equation (10) is as follows:

$$\begin{aligned}
& \left\| \frac{\partial \|\hat{\mathbf{w}}_i - \hat{\mathbf{w}}_j\|^{-s}}{\partial \mathbf{w}_i} \right\| \\
&= \left\| \frac{\partial \|\hat{\mathbf{w}}_i - \hat{\mathbf{w}}_j\|^{-s}}{\partial \|\hat{\mathbf{w}}_i - \hat{\mathbf{w}}_j\|} \frac{\partial \|\hat{\mathbf{w}}_i - \hat{\mathbf{w}}_j\|}{\partial (\hat{\mathbf{w}}_i - \hat{\mathbf{w}}_j)} \frac{\partial (\hat{\mathbf{w}}_i - \hat{\mathbf{w}}_j)}{\partial \hat{\mathbf{w}}_i} \frac{\partial \frac{\mathbf{w}_i}{\|\mathbf{w}_i\|}}{\partial \mathbf{w}_i} \right\| \\
&= \left\| \frac{s}{\|\hat{\mathbf{w}}_i - \hat{\mathbf{w}}_j\|^{s+1}} \frac{(\hat{\mathbf{w}}_i - \hat{\mathbf{w}}_j)^T}{\|\hat{\mathbf{w}}_i - \hat{\mathbf{w}}_j\|} I \frac{(I - M_{\mathbf{w}_i})}{\|\mathbf{w}_i\|} \right\| \\
&= \frac{\|s(I - M_{\mathbf{w}_i})\hat{\mathbf{w}}_j\|}{\|\mathbf{w}_i\| \|\hat{\mathbf{w}}_i - \hat{\mathbf{w}}_j\|^{s+2}} \\
&= \frac{s}{\|\mathbf{w}_i\|} \frac{\sin \theta_{ij}}{(2 \sin \frac{\theta_{ij}}{2})^{s+2}} \\
&= \frac{s}{\|\mathbf{w}_i\|} \frac{\cos \frac{\theta_{ij}}{2}}{(2 \sin \frac{\theta_{ij}}{2})^{s+1}}, \quad \text{with } M_{\mathbf{w}_i} = \frac{\mathbf{w}_i \mathbf{w}_i^T}{\|\mathbf{w}_i\|^2}
\end{aligned}$$

The detail derivation of Equation (12) is as follows:

$$\begin{aligned}
& \left\| \frac{\partial \log \|\hat{\mathbf{w}}_i - \hat{\mathbf{w}}_j\|}{\partial \mathbf{w}_i} \right\| \\
&= \frac{1}{\|\hat{\mathbf{w}}_i - \hat{\mathbf{w}}_j\|} \left\| \frac{\partial \|\hat{\mathbf{w}}_i - \hat{\mathbf{w}}_j\|^{-(-1)}}{\partial \mathbf{w}_i} \right\| \\
&= \frac{1}{\|\hat{\mathbf{w}}_i - \hat{\mathbf{w}}_j\|} \frac{|-1|}{\|\mathbf{w}_i\|} \frac{\cos \frac{\theta_{ij}}{2}}{(2 \sin \frac{\theta_{ij}}{2})^{-1+1}} \\
&= \frac{1}{\|\mathbf{w}_i\|} \frac{\cos \frac{\theta_{ij}}{2}}{(2 \sin \frac{\theta_{ij}}{2})}
\end{aligned}$$

B Dataset Description of Section 5

We conduct our image classification experiments on CIFAR100 [4] and TinyImageNet [5]. The CIFAR100 consists of 50k and 10k images of 32×32 pixels for the training and test sets respectively. We present experiments trained on the training set and evaluated on the test set. The TinyImageNet dataset is a subset of the ILSVRC2012 classification dataset [8]. It consists of 200 object classes, and each class has 500 training images, 50 validation images, and 50 test images. All images have been downsampled to 64×64 pixels. As the labels for test set are not released, we present experiments trained on the training set and evaluated on the validation set. For both datasets, we follow the simple data augmentation in [6]. For training, 4 pixels are padded on each side and a 32×32 crop for CIFAR100 or a 64×64 crop for TinyImageNet is randomly sampled from the padded image or its horizontal flip. For testing, we only evaluate the single view of the original 32×32 image for CIFAR100 or 64×64 image for TinyImageNet. Note that our focus is on the effectiveness of our proposed MMA regularization, not on pushing the state-of-the-art results, so we do not use any more data augmentation and training tricks to improve accuracy.

C Implementation Settings of Section 6

We employ CASIA [10] as training dataset and LFW [3], CFP-FP [9], and AgeDB-30 [7] as face verification datasets. For the embedding network, we employ ResNet50 [2]. The angular margin m is set to 0.5 according to the ArcFace paper [1]. The regularization coefficient λ is set to 0.03. Other hyperparameters and settings exactly follow the ArcFace paper [1], except for the batchsize and learning schedule. Due to the limit of hardware, we set the batch size to 440 (the ArcFace paper sets to 512). Accordingly, we finish the training process at 38K iterations and decay the learning rate by a factor of 10 at 23750 and 33250 iterations to ensure the same training samples.

D Supplement to Section 5.2: Comparison of the Minimal Pairwise Angle

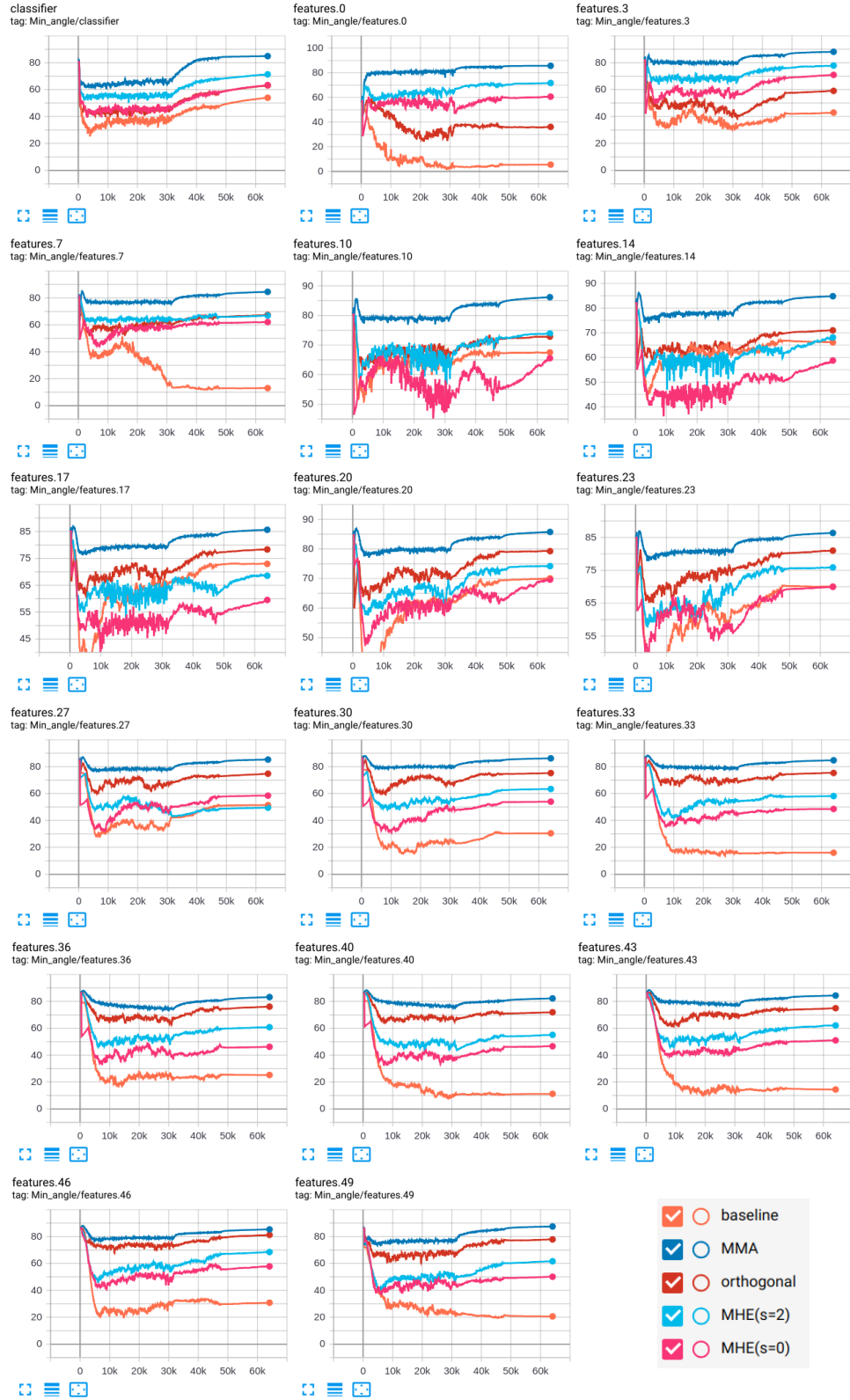


Figure 1: Comparison of the minimal pairwise angle from all layers of VGG19-BN trained on CIFAR100 with several different diversity regularization. The MMA regularization gets the largest minimal pairwise angle consistently across all layers, and therefore the most diverse weight vectors.

References

- [1] Jiankang Deng, Jia Guo, Niannan Xue, and Stefanos Zafeiriou. Arcface: Additive angular margin loss for deep face recognition. In *Proceedings of the IEEE Conference on Computer Vision and Pattern Recognition*, pages 4690–4699, 2019.
- [2] Kaiming He, Xiangyu Zhang, Shaoqing Ren, and Jian Sun. Deep residual learning for image recognition. In *Proceedings of the IEEE conference on computer vision and pattern recognition*, pages 770–778, 2016.
- [3] Gary B Huang, Marwan Mattar, Tamara Berg, and Eric Learned-Miller. Labeled faces in the wild: A database for studying face recognition in unconstrained environments. 2008.
- [4] Alex Krizhevsky and Geoffrey Hinton. Learning multiple layers of features from tiny images. Technical report, Citeseer, 2009.
- [5] Ya Le and Xuan Yang. Tiny imagenet visual recognition challenge. *CS 231N*, 2015.
- [6] Chen-Yu Lee, Saining Xie, Patrick Gallagher, Zhengyou Zhang, and Zhuowen Tu. Deeply-supervised nets. In *Artificial Intelligence and Statistics*, pages 562–570, 2015.
- [7] Stylianos Moschoglou, Athanasios Papaioannou, Christos Sagonas, Jiankang Deng, Irene Kotsia, and Stefanos Zafeiriou. Agedb: the first manually collected, in-the-wild age database. In *Proceedings of the IEEE Conference on Computer Vision and Pattern Recognition Workshops*, pages 51–59, 2017.
- [8] Olga Russakovsky, Jia Deng, Hao Su, Jonathan Krause, Sanjeev Satheesh, Sean Ma, Zhiheng Huang, Andrej Karpathy, Aditya Khosla, Michael Bernstein, et al. Imagenet large scale visual recognition challenge. *International journal of computer vision*, 115(3):211–252, 2015.
- [9] Soumyadip Sengupta, Jun-Cheng Chen, Carlos Castillo, Vishal M Patel, Rama Chellappa, and David W Jacobs. Frontal to profile face verification in the wild. In *2016 IEEE Winter Conference on Applications of Computer Vision (WACV)*, pages 1–9. IEEE, 2016.
- [10] Dong Yi, Zhen Lei, Shengcai Liao, and Stan Z Li. Learning face representation from scratch. *arXiv preprint arXiv:1411.7923*, 2014.